

Elastoplastic Behavior of AA2124 Alloy used to make Hemispherical Cups

Teniya Choppala¹, A. Chennakesava Reddy²

¹PG Student, JNT University, Hyderabad – 500 085, Telangana, India

²Professor, JNT University, Hyderabad – 500 085, Telangana, India

Abstract: The objective of the current work was to estimate plastic behavior of AA2124 alloy to manufacture hemispherical cups. The design procedure for the finite element analysis was carried out as per Taguchi's techniques using ABAQUS software code. The tool radius of incremental deep drawing was the critical process parameter influencing the effective stress induced during the formation of hemispherical cups. von Mises stresses induced in the cups are within the limit of ultimate strength of AA2124. The sheet thickness and step depth had influenced the reduction of sheet thickness during the cup formation.

Keywords: Hemispherical cups, AA2124 alloy, finite element analysis, single-point incremental forming process

1. Introduction

The necessity of making mechanically sound objects with high functional performance which can withstand stresses like tensile, compression or combined stresses in manufacturing industry has led to creation of forming process. In conventional forming process a sheet metal blank is radially drawn into a forming die by the mechanical action of a punch. The incremental sheet forming (figure 1) has the advantage of forming in lesser time and more complicated shapes at lower cost than the conventional process. Among many simulation software used for Finite Element Analysis (FEA) and Computer Aided Engineering (CAE), ABAQUS is popular due to the wide material modeling capability, and the program's ability to be customized.

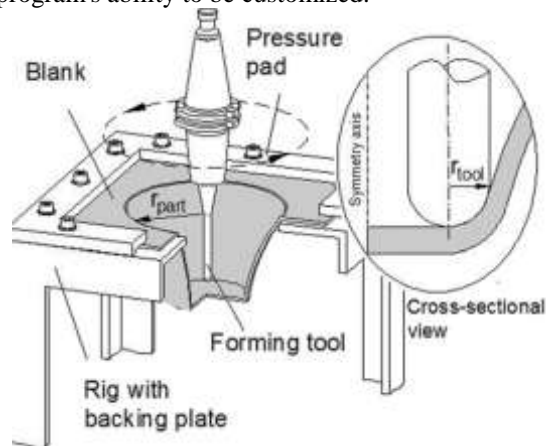


Figure 1: Single point incremental forming process

In a series of research on deep drawing process, a rich investigation have been carried out on warm deep drawing process to improve the super plastic properties of materials such as AA1050 alloy [1], [2], [3], [4], [5], [6], AA2014 alloy [7], AA2017 alloy [8], AA2024 alloy [9], AA2219 alloy [10], AA2618 alloy [11], AA3003 alloy [12], AA5052 alloy [13], AA5049 alloy [14], AA5052 alloy [15], AA6061 alloy [16], Ti-Al-4V alloy [17], EDD steel [18], gas cylinder steel [19]. Also, different cup shapes such as pyramidal [2, 16], rectangular [3, 17] and cone [4, 18] were fabricated. The process parameters which influence incremental sheet form-

ing are many parameters which affect the process mainly step depth, tool diameter, sheet thickness, friction coefficient, type of lubricant, tool path, increments along X and Y directions, spindle speed, feed rate, wall angle [20,21]. Malwad et al. [22] described the deformation mechanism by variation of wall angles. Greater formability can be achieved in cups which have wall angle less than 75°. As the wall angle reduces shearing plays an important role in deformation and biaxial stretching takes place at the corners so the sheet cracks at corners rather than sides. The numerical simulations of frustum of cone and pyramid with different slope angles were performed using LS-DYNA and analyzed the formability. The objective of the present work was to estimate the formability of AA2124 alloy to fabricate hemispherical cups using single point incremental deep drawing process. Finite element analysis (FEA) was implemented to estimate various process parameters of deep drawing process.

2. Material and Methods

AA2124 alloy sheet was used in this study of single point incremental sheet forming to fabricate hemispherical cups. The composition of AA2124 alloy is given in Table 1. The mechanical properties of AA2124 alloy are given in Table 2.

Table 1: Chemical composition of AA2124 alloy

Element	% weight
Aluminium	93.18
Copper	4.31
Magnesium	1.29
Manganese	0.81
Iron	0.19
Chromium	0.08
Silicon	0.07
Zinc	0.07

Table 2: Mechanical properties of AA 2124 alloy

Density	2780 kg/m ³
Yield strength	441 MPa
Poisson's ratio	0.33
Modulus of elasticity	73.1 GPa

Plasticity data was obtained by conducting tensile test of AA 2124 alloy, from which the data is represented in figure 2. The obtained values were taken as material properties-plasticity for simulation of SPIF process.

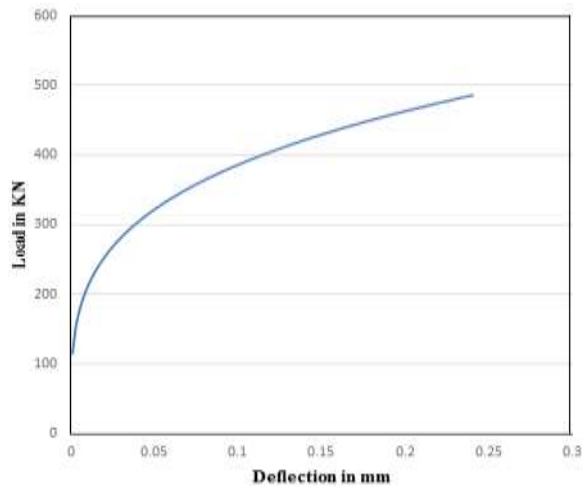


Figure 2: Load vs. Deflection of AA 2124 alloy.

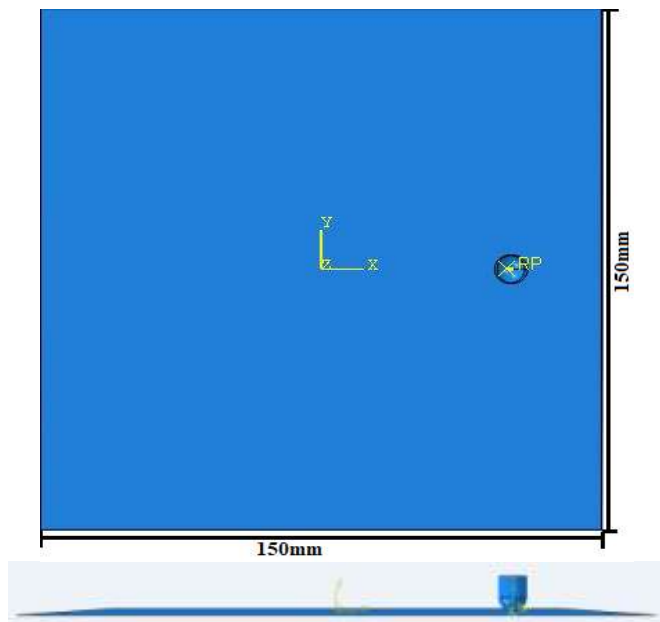


Figure 3: Modeled sheet and Tool.

The finite element method (FEM) has become an important tool for the numerical solutions of engineering problems. It is the piecewise approximation of object where the object is divided into number of small elements, the integration of all such small elemental analysis finally give the solutions [23]. The finite element modeling of SPIF process was carried out using ABAQUS (6.14) software to fabricate hemispherical cups. In geometric modelling a square sheet of dimensions 150 mm×150 mm and tool of cylindrical rod hemispherical end was created as mentioned in Table 3. The sheet and tool were modelled as deformable, analytical rigid body respectively and assembled together as shown in figure 3. In order to reduce the complexity of the model the other parts like tool holder, work holder were simulated by boundary conditions, hence this is a simplified model. Tool was given a reference point for governing tool motion. Contact was the interaction between tool and the sheet. Since the sheet undergoes the localized deformation at the contact, modelling of contact

should be correct. The contact was modelled as frictional contact. Coefficient of friction was considered at different levels as per design of experiments in Table 3.

Meshing is the process of discretizing the component. Here the sheet was meshed as shown in figure 4 with quad dominated S4R shell elements [24]. Element size has impact on computational time and results. Fine mesh gives the good results with greater computational time. Coarse mesh leads to inconsistent results, penetration and convergence problems during simulation process. A fine mesh of 2mm was generated for consistent results.

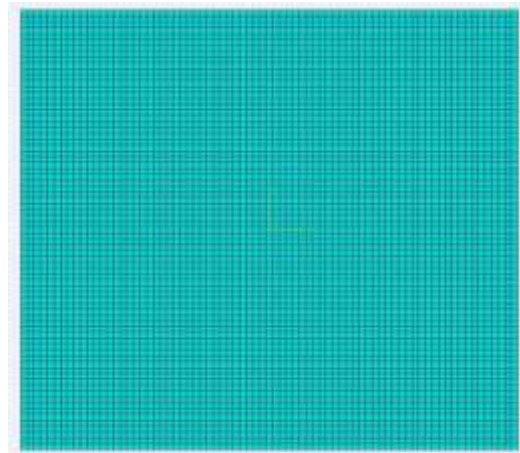


Figure 4: Meshed sheet.

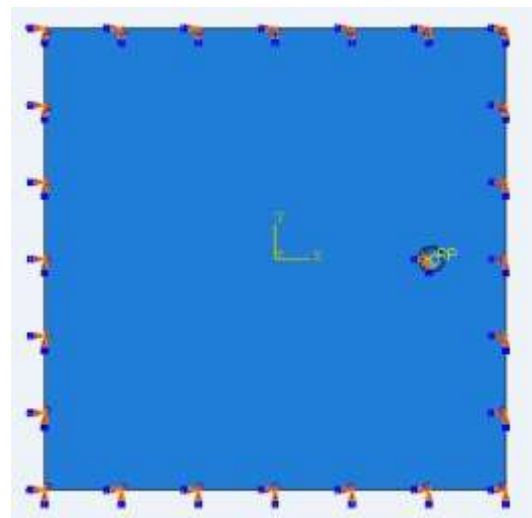


Figure 5: Boundary Conditions.

A simplified model was created by eliminating tool holder and work holder, but they are simulated by the boundary conditions. Edges of the sheet are fixed and tool was given four degrees of freedom, three translatory along x, y, z directions and one rotational around tool axis as shown in figure 5. The motion of the tool was controlled by amplitude data in smooth step form. The tool path generated by the CAM package [24] for hemispherical cup is as shown in the figure 6.

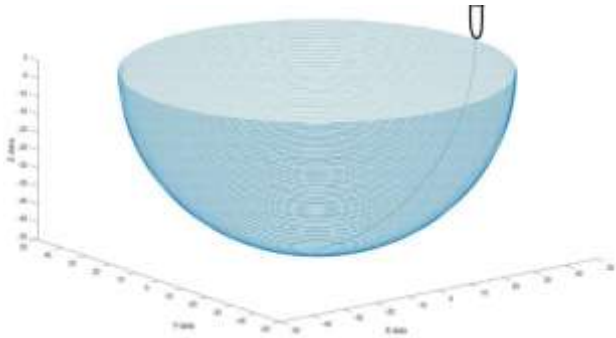


Figure 6: Tool path profile.

The finite element analysis was carried out as per Taguchi's techniques. The levels of process parameters are given in Table 3. The assignment of process parameters is given in Table 4.

Table 3: Process Parameters and levels

Factor	Symbol	Level-1	Level-2	Level-3
Sheet thickness, (mm)	A	0.8	1	1.2
Step depth, (mm)	B	0.5	0.75	1
Tool radius, (mm)	C	4	6	8
Coefficient of friction	D	0.05	0.1	0.15

Table 4: Orthogonal array (L9) and control parameters

Trial No.	A	B	C	D
1	1	1	1	1
2	1	2	2	2
3	1	3	3	3
4	2	1	2	3
5	2	2	3	1
6	2	3	1	2
7	3	1	3	2
8	3	2	1	3
9	3	3	2	1

3. Results and Discussion

The maximum equivalent stresses induced in the hemispherical cups are 397.0976, 315.266, 350.779, 379.256, 309.913, 395.071, 342.075, 399.579 and 326.466MPa for trials 1 to 9 (figures 7-9) respectively. Maximum equivalent stress is observed in the walls of cup of trial 8. Corresponding maximum equivalent plastic strain obtained for trials 1 to 9 are 3.449, 3.248, 3.393, 3.131, 3.359, 3.407, 3.161, 3.5997 and 3.437; it is observed maximum equivalent plastic strain in the walls of cup 8.

The strain variation along the wall of hemispherical cup at respective step depths is shown in figure 10. The tool radius (C) of incremental deep drawing has maximum influence of 69% on the plastic deformation of cups. The friction coefficient (D) has also influenced to the extent of 16%. The step depth (B) has contributed to the extent of 14%. The sheet thickness did not influence the plastic deformation of the cups.

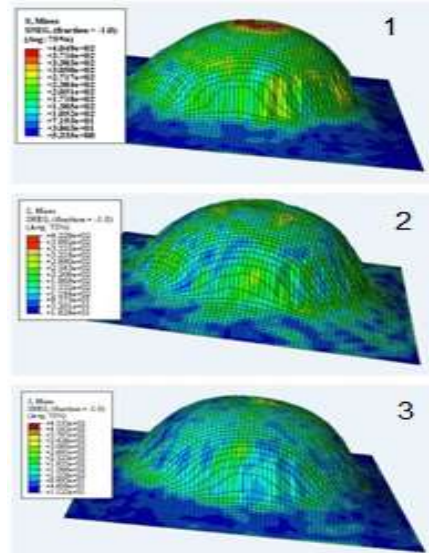


Figure 7: Equivalent stress induced in sheet thickness of 0.8 mm.

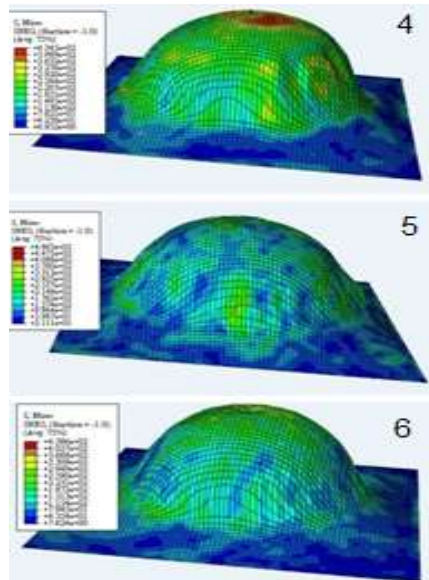


Figure 8: Equivalent stress induced in sheet thickness of 1.0 mm.

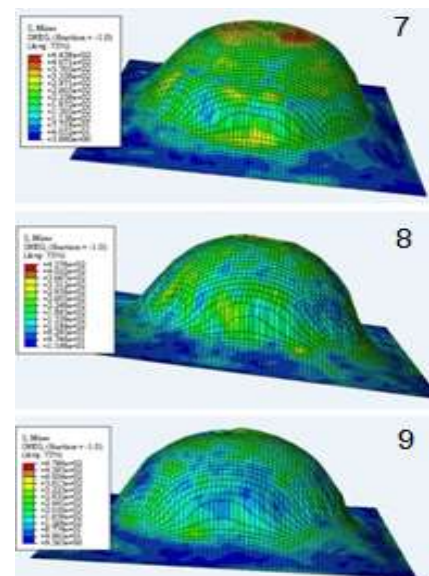


Figure 9: Equivalent stress induced in sheet thickness of 1.2 mm.

The variation of sheet thickness along the walls of the cup is shown in figure 11. It is also observed that the reduction in wall thickness of the cups is greatly influenced by the sheet thickness (A) and step depth (B) of incremental deep drawing process to the extent of 63.62% and 31.81% respectively. The other process had no effect on the reduction of sheet thickness as mentioned in Table 5.

hemispherical cups. The ultimate strength of AA2124 alloy is 483 MPa. All the trial conditions are in the safe limits of AA2124 alloy.

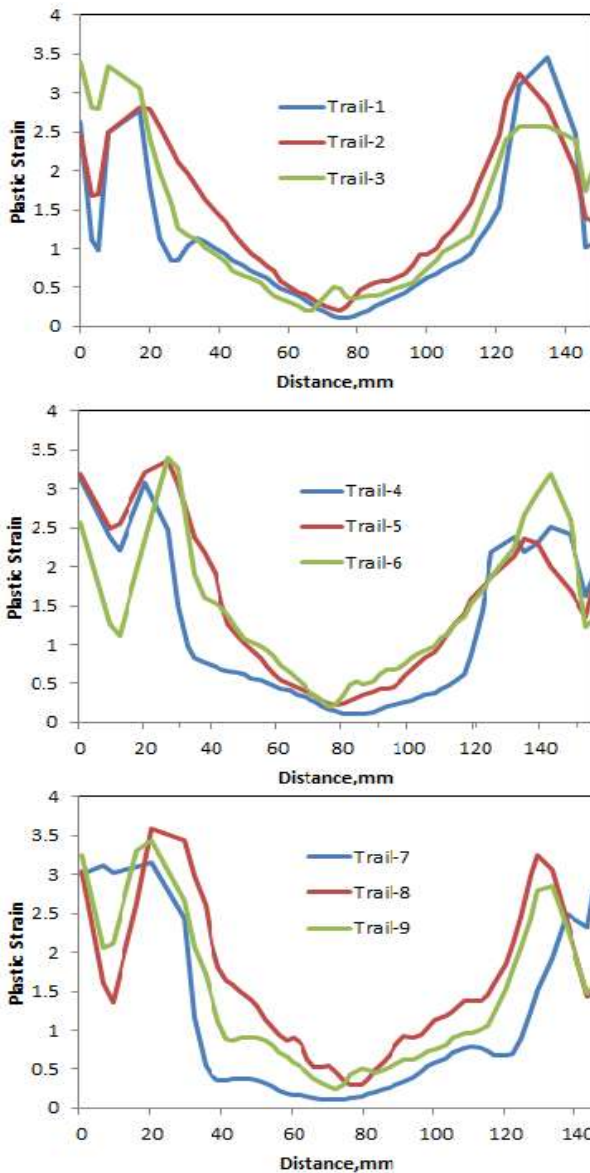


Figure 10: Plastic strain induced along the walls of cup.

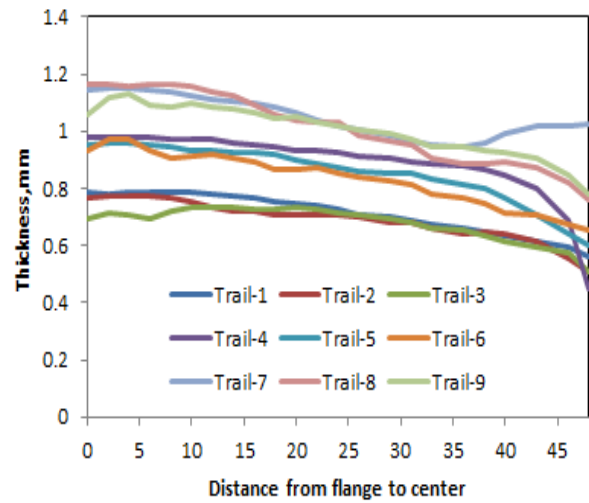


Figure 11: Variation of sheet thickness along the walls of cup.

Table 5: ANOVA analysis of thickness reduction

Factor	S1	S2	S3	SS	v	V	F	P
A	0.65	0.88	1.02	0.02	1	0.02	13.92	63.62
B	0.75	0.90	0.90	0.01	1	0.01	6.96	31.81
C	0.82	0.85	0.88	0.00	1	0.00	0.00	0.00
D	0.89	0.82	0.84	0.00	1	0.00	0.00	0.00
e				0.00	4	0.00	0.00	4.57
T	3.10	3.46	3.63	0.03	8			100.00

Table 4: ANOVA analysis of equivalent stress

Factor	S1	S2	S3	SS	v	V	F	P
A	1063	1084	1068	81	1	81	6704	1
B	1118	1025	1072	1462	1	1462	120921	14
C	1192	1021	1003	7245	1	7245	599013	69
D	1033	1052	1130	1729	1	1729	142959	16
e				0	4	0	0	0
T	4407	4182	4273	10517	8			100

The hemispherical and its cut-section is shown in figure 12. The stress-based formability diagrams of the cups are shown in figures 13(a), 13(b) and 13(c). The formability of the hemispherical cups is dominated by the compressive stress. The lowest and highest von Mises stresses are respectively 309.913 and 399.579 MPa for the trails 5 and 8 of the

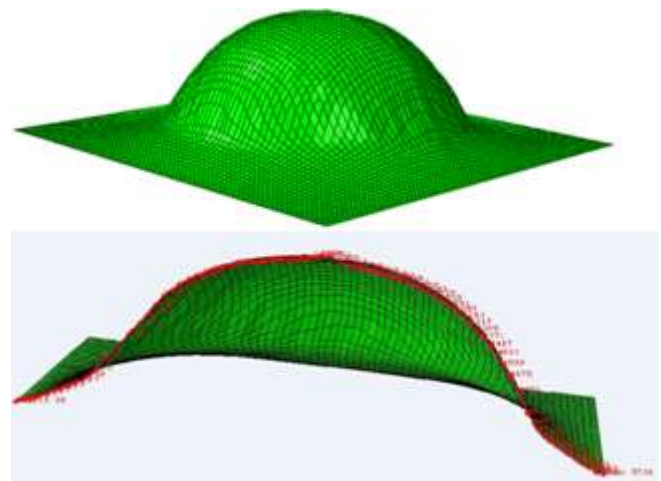
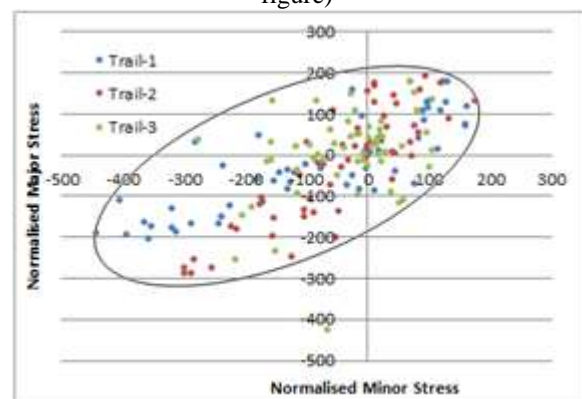


Figure 12: Formation of hemispherical cup. (you change figure)



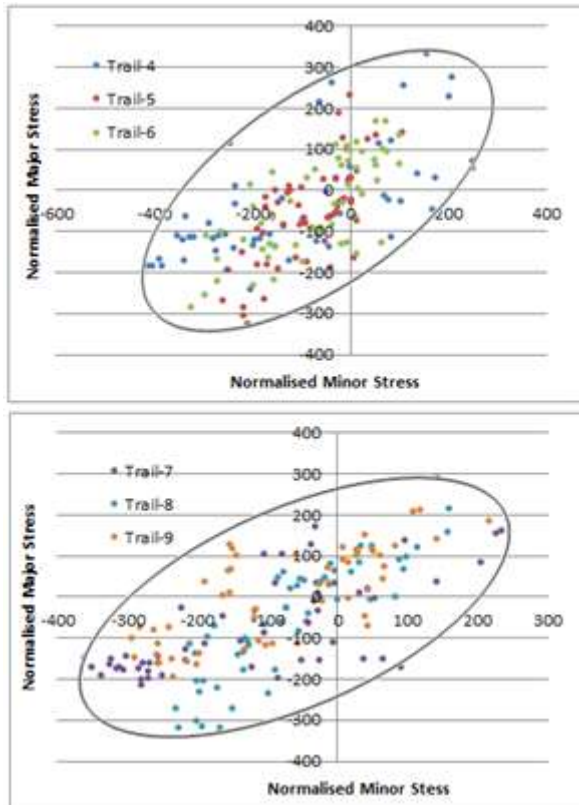


Figure 13: Formability of hemispherical cups.

4. Conclusions

The finite element analysis was carried out as per Taguchi's techniques using ABAQUS software code. The tool radius (C) of incremental deep drawing has maximum influence on the effective stress induced in the hemispherical cups to the extent of 69%. The sheet thickness and step depth had influenced the reduction of sheet thickness during the cup formation. The lowest and highest von Mises stresses respectively 309.913 and 399.579 MPa for the trails 5 and 8 of the hemispherical cups are within the limits of the ultimate strength of AA2124 (483 MPa).

References

- [1] A. C. Reddy, Homogenization and Parametric Consequence of Warm Deep Drawing Process for 1050A Aluminum Alloy: Validation through FEA, *International Journal of Science and Research*, vol. 4, no. 4, pp. 2034-2042, 2015.
- [2] A. C. Reddy, Formability of Warm Deep Drawing Process for AA1050-H18 Pyramidal Cups, *International Journal of Science and Research*, vol. 4, no. 7, pp. 2111-2119, 2015.
- [3] A. C. Reddy, Formability of Warm Deep Drawing Process for AA1050-H18 Rectangular Cups, *International Journal of Mechanical and Production Engineering Research and Development*, vol. 5, no. 4, pp. 85-97, 2015.
- [4] A. C. Reddy, Formability of superplastic deep drawing process with moving blank holder for AA1050-H18 conical cups, *International Journal of Research in Engineering and Technology*, vol. 4, no. 8, pp. 124-132, 2015.
- [5] A. C. Reddy, Performance of Warm Deep Drawing Process for AA1050 Cylindrical Cups with and Without Blank Holding Force, *International Journal of Scientific Research*, vol. 4, no. 10, pp. 358-365, 2015.
- [6] A. C. Reddy, Necessity of Strain Hardening to Augment Load Bearing Capacity of AA1050/AlN Nanocomposites, *International Journal of Advanced Research*, vol. 3, no. 6, pp. 1211-1219, 2015.
- [7] A. C. Reddy, Parametric Optimization of Warm Deep Drawing Process of 2014T6 Aluminum Alloy Using FEA, *International Journal of Scientific & Engineering Research*, vol. 6, no. 5, pp. 1016-1024, 2015.
- [8] A. C. Reddy, Finite Element Analysis of Warm Deep Drawing Process for 2017T4 Aluminum Alloy: Parametric Significance Using Taguchi Technique, *International Journal of Advanced Research*, vol. 3, no. 5, pp. 1247-1255, 2015.
- [9] A. C. Reddy, Parametric Significance of Warm Drawing Process for 2024T4 Aluminum Alloy through FEA, *International Journal of Science and Research*, vol. 4, no. 5, pp. 2345-2351, 2015.
- [10] A. C. Reddy, Formability of High Temperature and High Strain Rate Superplastic Deep Drawing Process for AA2219 Cylindrical Cups, *International Journal of Advanced Research*, vol. 3, no. 10, pp. 1016-1024, 2015.
- [11] C. R. Alavala, High temperature and high strain rate superplastic deep drawing process for AA2618 alloy cylindrical cups, *International Journal of Scientific Engineering and Applied Science*, vol. 2, no. 2, pp. 35-41, 2016.
- [12] C. R. Alavala, Practicability of High Temperature and High Strain Rate Superplastic Deep Drawing Process for AA3003 Alloy Cylindrical Cups, *International Journal of Engineering Inventions*, vol. 5, no. 3, pp. 16-23, 2016.
- [13] C. R. Alavala, High temperature and high strain rate superplastic deep drawing process for AA5049 alloy cylindrical cups, *International Journal of Engineering Sciences & Research Technology*, vol. 5, no. 2, pp. 261-268, 2016.
- [14] C. R. Alavala, Suitability of High Temperature and High Strain Rate Superplastic Deep Drawing Process for AA5052 Alloy, *International Journal of Engineering and Advanced Research Technology*, vol. 2, no. 3, pp. 11-14, 2016.
- [15] C. R. Alavala, Development of High Temperature and High Strain Rate Superplastic Deep Drawing Process for 5656 Al-Alloy Cylindrical Cups, *International Journal of Mechanical and Production Engineering*, vol. 4, no. 10, pp. 187-193, 2016.
- [16] C. R. Alavala, Effect of Temperature, Strain Rate and Coefficient of Friction on Deep Drawing Process of 6061 Aluminum Alloy, *International Journal of Mechanical Engineering*, vol. 5, no. 6, pp. 11-24, 2016.
- [17] A. C. Reddy, Finite element analysis of reverse superplastic blow forming of Ti-Al-4V alloy for optimized control of thickness variation using ABAQUS, *Journal of Manufacturing Engineering, National Engineering College*, vol. 1, no. 1, pp. 6-9, 2006.
- [18] A. C. Reddy, T. Kishen Kumar Reddy, M. Vidya Sagar, Experimental characterization of warm deep drawing process for EDD steel, *International Journal of Multidisciplinary Research & Advances in Engineering*, vol. 4, no. 3, pp. 53-62, 2012.

- [19] A. C. Reddy, Evaluation of local thinning during cup drawing of gas cylinder steel using isotropic criteria, International Journal of Engineering and Materials Sciences, vol. 5, no. 2, pp. 71-76, 2012.
- [20] J. Kopac and Z. Kampus, Incremental sheet metal forming on CNC milling machine-tool, 13 International Science Conference on Achievement in Mechanical and Materials Engineering, 2005.
- [21] K. Suresh, A. Khan, R. Srinivasa Prakash, Tool path definition for numerical simulation of single point incremental forming, Procedia Engineering, vol. 64, pp. 536 – 545, 2013.
- [22] D. S. Malwad, V. M. Nandedkar, Deformation Mechanism Analysis of Single Point Incremental Sheet Metal Forming Procedia Materials Science, vol. 6, pp. 1505 – 1510, 2014.
- [23] C. R. Alavala, Finite element methods: Basic Concepts and Applications, PHI Learning Pvt. Ltd., 2008.
- [24] C. R. Alavala, CAD/CAM: Concepts and Applications, PHI Learning Pvt. Ltd, 2008.